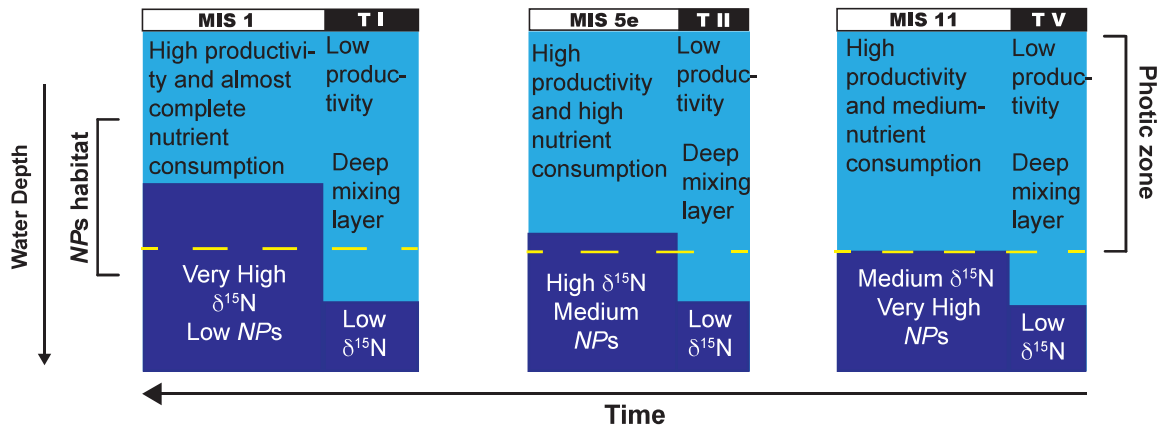


## **Highlights**

- A thin mixed-layer and a strongly stratified upper-water characterized MIS1
- A thick mixed-layer prevailed during MIS11 and reduced nitrate utilization
- These contrasting results explain the weak expression of MIS11 in the polar latitudes
- Caution is needed when using older interglacials as near-future climate analogues



1 **Stratification-induced variations in nutrient utilization in the Polar North**  
2 **Atlantic during past interglacials**

3

4 **Authors:** Benoit Thibodeau<sup>1,2,5\*</sup>, Henning A Bauch<sup>3,4,5</sup>, Thomas F Pedersen<sup>6</sup>

5 **Affiliations:**

6 <sup>1</sup>Department of Earth Sciences, The University of Hong Kong, Pokfulam Road, Hong Kong  
7 SAR

8 <sup>2</sup>Swire Institute for Marine Science, The University of Hong Kong, Cape d'Aguilar Road,  
9 Shek O, Hong Kong SAR

10 <sup>3</sup>Alfred-Wegener-Institute for Polar and Marine Research, Columbusstrasse, 27568  
11 Bremerhaven, Germany

12 <sup>4</sup> GEOMAR - Helmholtz Centre for Ocean Research, Wischhofstrasse 1-3, 24148 Kiel,  
13 Germany

14 <sup>5</sup>Academy of Science, Humanities and Literature, Geschwister-Schollstrasse 2, 55131 Mainz,  
15 Germany

16 <sup>6</sup>School of Earth and Ocean Sciences, Bob Wright Centre, University of Victoria  
17 3800 Finnerty Road, Victoria, BC, V8P 5C2, Canada

18

19 \*Correspondence to: Benoit Thibodeau, Department of Earth Sciences, University of Hong  
20 Kong, Pokfulam Road, Hong Kong SAR +852 3917 7834 [bthib@hku.hk](mailto:bthib@hku.hk)

21

22 Keywords: Stratification, Polar Seas, Global changes, Atlantic Meridional Overturning

23 Circulation, freshwater discharge

24

25 **Abstract:** Vertical water mass structure in the Polar North Atlantic Ocean plays a critical role  
26 in planetary climate by influencing the formation rate of North Atlantic deepwater, which in  
27 turn affects surface heat transfer in the northern hemisphere, ventilation of the deep sea, and  
28 ocean circulation on a global scale. However, the response of upper stratification in the  
29 Nordic seas to near-future hydrologic forcing, as surface water warms and freshens due to  
30 global temperature rise and Greenland ice demise, remains poorly known. While past major  
31 interglacials are viewed as potential analogues of the present, recent findings suggest that  
32 very different surface ocean conditions prevailed in the Polar North Atlantic during Marine  
33 Isotope Stage (MIS) 5e and 11 compared to the Holocene. It is thus crucial to identify the  
34 causes of those differences in order to understand their role in climatic and oceanographic  
35 variability. To resolve this, we pair here bulk sediment  $\delta^{15}\text{N}$  isotopic signatures with  
36 planktonic foraminiferal assemblages and their isotopic composition across major past  
37 interglacials. The comparison defines for the first time stratification-induced variations in  
38 nitrate utilization up to 25% between and within all of these warm periods that highlight  
39 changes in the thickness of the mixed-layer throughout the previous interglacials. That  
40 thickness directly controls the depth-level of Atlantic water inflow. The major changes of  
41 nitrate utilization recorded here thus suggest that a thicker mixed-layer prevailed during past  
42 interglacials, probably related to longer freshwater input associated with the preceding glacial  
43 termination. This would have caused the Atlantic water to flow at greater depth during MIS  
44 5e and 11. These results call for caution when using older interglacials as modern or near-  
45 future climate analogues and contribute to the improvement of our general comprehension of  
46 the impact of freshwater input near a globally important deep-water formation site like the  
47 Nordic Seas. This is crucial when assessing the negative impacts on the Greenland Ice Sheet  
48 of climate change and global warming.

49

## 50 **1. Introduction**

51 Deepwater convection in the Nordic Seas relies on the inflow of warm, saline upper-  
52 ocean waters from the Atlantic. These gradually increase in density and sink as the waters  
53 move northward and cool (Hansen and Østerhus, 2000; Isachsen et al., 2007; Lohmann et al.,  
54 2014; Mauritzen, 1996; Swift and Aagaard, 1981). This convective process profoundly  
55 affects surface heat transfer in the northern hemisphere, ventilation of the deep sea, and ocean  
56 circulation on a global scale (Clark et al., 2002; Vellinga and Wood, 2002). While the general  
57 convective pattern differed during past glacial intervals and ensuing terminations (Lynch-  
58 Stieglitz et al., 2007), convection and deep ocean circulation during interglacials is thought to  
59 have been similar to that today (Bohm et al., 2015). However, it has been suggested that  
60 climatic and oceanic instabilities could have led to relatively abrupt variations in the strength  
61 of North Atlantic Deep Water (NADW) formation during the last interglacial (Marine Isotope  
62 Stage [MIS] 5e) and its associated termination (e.g., Fronval and Jansen, 1996; Galaasen et  
63 al., 2014; Seidenkrantz et al., 1995). In most cases NADW reduction events are thought to  
64 have been triggered by deglacial ice-sheet melting and sudden freshwater releases that  
65 rendered the surface water denser, thus altering the upper-ocean stratification at convection  
66 sites. While such events are considered to play a crucial role on planetary climate by  
67 influencing the strength of the Atlantic meridional overturning circulation (AMOC)  
68 (Rahmstorf, 2002; Rahmstorf et al., 2015), their frequency and estimated intensity remain  
69 poorly constrained beyond the Last Glacial Maximum, some 21,000 years ago. Since both  
70 warming and freshening of the Polar North Atlantic are expected during the next century  
71 (Dickson et al., 2007; Glessmer et al., 2014; Kirtman et al., 2013; Peterson et al., 2006),  
72 determining the sensitivity of upper water stratification in the Nordic Seas during pre-  
73 Holocene interglacial periods—when global temperatures were likely higher than today—

74 offers a way to forecast the impact of the warmer climate that greenhouse gas emissions are  
75 driving us toward.

76 Two key analogues of impending climate states are the Eemian or last interglaciation  
77 (MIS 5e) and the Holsteinian or Hoxnian (MIS 11), respectively centered around 125 ka and  
78 400 ka. Both appear to represent near-future climate conditions that are similar to model  
79 projections for the end of this century: warmer-than-Holocene temperatures (+ 5°C) over  
80 most of Europe (Kaspar, 2005; Otto-Bliesner et al., 2006) and the Arctic, and widely reduced  
81 sea-ice cover (CAPE Last Interglacial Project Members, 2006). Moreover, the Holocene and  
82 the Holsteinian share similar orbital forcing characteristics (insolation) and initial greenhouse  
83 gas concentrations (Berger and Loutre, 1991; EPICA community members, 2004). Despite  
84 such overall similarities, growing evidence suggests that interactions between glacial ice-  
85 sheet size, deglaciation-specific traits and post-glacial sea level rise largely determine the  
86 water mass structure and climate (Bauch, 2013; Vázquez Riveiros et al., 2013). This is well  
87 illustrated by the cooler-than-Holocene reconstructed sea surface temperature in the Nordic  
88 Seas during both MIS 5e and 11 (Kandiano et al., 2012; Van Nieuwenhove et al., 2011) (Fig.  
89 1). While the specifics of each period do not inhibit the unravelling of key influences on  
90 present and future climate, they call for caution when trying to understand important  
91 processes that drive the AMOC and heat delivery to the Polar region. It is therefore critical  
92 to evaluate independently the properties of upper ocean structure in the Polar North Atlantic  
93 during each analogue interval if we are to comprehend better the potential of past warm  
94 periods to act as exemplars for modern or near-future climate.

95 The modern upper-ocean structure of the Nordic Seas is dictated by seasonality.  
96 Surface water is well stratified during summer with a mixed-layer thinner than 30 m  
97 (Jeansson et al., 2015). The mixed-layer is thus well above the light penetration depth, which  
98 allow a near complete consumption of surface nitrate during this period (Fig 2a). During

99 winter the cooling of salty Atlantic-derived surface water promotes deeper mixing, creating a  
100 mixed-layer that can reach up to 300 m in thickness (Fig 2b; Jeansson et al., 2015). This  
101 process is crucial in the formation of deep-water and to the replenishment of nitrate to surface  
102 water (Jeansson et al., 2015; Swift and Aagaard, 1981).

103         Reconstructing upper ocean water mass structure in Polar regions is not  
104 straightforward due to the difficulty in estimating mixed-layer thickness. Here, we propose a  
105 novel approach that overcomes this constraint, using the abundance of the polar water  
106 indicator foraminiferal species *Neogloboquadrina pachyderma* sinistral (*NPs*) in combination  
107 with the nitrogen isotopic composition of the host bulk sediment ( $\delta^{15}\text{N}_{\text{bulk}}$ ). The isotopic  
108 signature of nitrate in subpolar and polar water surface waters is controlled by the degree of  
109 nitrate utilization (Schubert et al., 2001). Relative utilization affects the  $\delta^{15}\text{N}$  of sinking  
110 particles; when nitrate is abundant (low relative utilization, and discrimination by  
111 phytoplankton against heavy nitrate) in the mixed layer, exported particulate organic matter is  
112 isotopically light. But when stratification inhibits mixing of “new” nitrate from below into  
113 the photic zone, relative nitrate utilization is higher and the exported particle flux is  
114 isotopically heavier (higher  $\delta^{15}\text{N}$ ). In the subpolar North Atlantic the degree of relative  
115 utilization is controlled by the thickness of the mixed-layer and thus by the stratification of  
116 the upper water column (Straub et al., 2013b). A well-stratified upper water column (thus,  
117 thin mixed layer) in spring and summer will limit the nitrate flux to the photic zone during  
118 growth season, resulting in high utilization and high  $\delta^{15}\text{N}$  of exported organic material, while  
119 a mixed-layer that extends below the photic zone during the same period will induce light  
120 limitation at depth and decrease nitrate utilization, leading to a lower aggregated  $\delta^{15}\text{N}$  in  
121 sinking particles (Fig. 3). Coherent to the light limitation, a thick cold and fresh mixed-layer  
122 might hypothetically reduce the growth season by delaying the spring ice breakup, which  
123 could reinforce the decrease in nitrogen utilization. The  $\delta^{15}\text{N}$  of sinking particles can also be



124 affected by an increase in nitrate supply, which, taken alone, would tend to lower the nitrate  
125 utilization. However, since nitrate is fully utilized by the end of the summer (Jeansson et al.,  
126 2015), increased input would support an increase in primary productivity, which would have  
127 the opposite effect on utilization (Galbraith et al., 2008) and thus the final effect on the nitrate  
128 utilization would be minimal. Despite the influence of nitrate input and productivity being  
129 probably minimal on the nitrate utilization, we used the abundance of polar foraminiferal  
130 specie *Neogloboquadrina pachyderma* sinistral (*NPs*) to strengthen our interpretation of the  
131 mixed-layer depth. This species has been widely used as an inverse-indicator of Atlantic  
132 water in the Nordic Seas (e.g., Bauch et al., 1999). The abundance of *NPs* thus provides us  
133 with a qualitative estimate of the proportion of Polar and Atlantic water present between 0  
134 and 100m, which is the preferred depth habitat for this species (Pados and Spielhagen, 2014).  
135 This implies that under a thin summer mixed-layer the *NPs* abundance will be diminished  
136 compared to a summer characterized by a thicker mixed-layer (Fig 3). Thus concurrent low  
137  $\delta^{15}\text{N}$  values and high *NPs* numbers are interpreted as indicating a thick-mixed layer  
138 originating from fresh and cold water inputs that limit nutrient utilization (Fig 3). This  
139 approach allows temporal variations in nitrate utilization to be traced, and it therefore defines  
140 the mixed-layer depth and the past surface and subsurface vertical water mass structure of the  
141 Nordic Sea.

142

## 143 2. **Materials and Methods**

144 We used a well-dated sediment core from the central Nordic Seas (PS1243,  
145 69°22N/6°32W, 2710m water depth) to investigate surface water stratification over three  
146 specific intervals. The core chronostratigraphy was established based on the AMS-  
147 radiocarbon dated upper section of the core and cross correlation of benthic  $\delta^{18}\text{O}$ , carbonate  
148 content and sediment reflectance (Bauch et al., 2001). The three specific intervals of interest

149 cover the deglacial terminal phases (Termination I, II, and V), the complete interglacials of  
150 the Holocene, Eemian, and Holsteinian, as well as the ensuing post-interglacial periods of  
151 glacial inception. This site registers the intrusion of warm, saline Atlantic Water northward to  
152 the Polar North Atlantic and ultimately the Arctic Ocean (Fig. 4). Interglacial intervals are  
153 clearly identifiable within the core by an absence of iceberg-rafted debris (IRD), depleted  
154 planktic foraminiferal  $\delta^{18}\text{O}$  and lowered *Neogloboquadrina pachyderma* sinistral (NPs)  
155 abundance (Fig. 5). Records of  $\delta^{15}\text{N}$ , NPs and IRD covering those three intervals are scarce  
156 in this region mainly due to the low sedimentary nitrogen content. Between 300 and 500  
157 foraminifers were counted in the  $>125\mu\text{m}$  fraction of washed sediment. Ice-rafted-debris was  
158 counted in the size fraction  $>250\mu\text{m}$ . Carbonate content and mass accumulation rate of  
159 carbonate are presented as they are considered proxy of productivity in this region (Bauch et  
160 al., 2001). For each oxygen isotope analysis about 28 similar-sized specimens of the polar  
161 planktic foraminifer *Neogloboquadrina pachyderma* sinistral were taken from the 125-250  
162  $\mu\text{m}$  size fraction. Isotope measurements were performed at the Leibniz-Laboratory (Kiel  
163 University) on a Finnigan MAT 251 mass spectrometer combined with an automated  
164 carbonate preparation device. The analytical precision of the MAT 251 system was  $\pm 0.08\text{‰}$   
165 for  $\delta^{18}\text{O}$  based on multiple measurements of an internal standard. Most of the  $\delta^{18}\text{O}$  data  
166 presented in this paper have been previously published, but the bulk-sediment nitrogen  
167 isotopic data are new and are used here to assess, for the first time, the thickness of the  
168 mixed-layer.

169

### 170 2.1. Nitrogen Isotope measurement

171 The bulk  $\delta^{15}\text{N}$  measurements were performed at the Department of Earth and Ocean  
172 Sciences at the University of British Columbia. The N isotopic composition was analyzed  
173 using a Carlo-Erba CHN analyzer coupled to a VG prism mass spectrometer. The  $\delta^{15}\text{N}$  values

174 are reported relative to air N<sub>2</sub> with an analytical precision of ±0.2‰ based on multiple  
175 measurements of an acetanilide internal standard.

176

### 177 **3. Results**

#### 178 *3.1. Bulk $\delta^{15}N$*

179 The  $\delta^{15}N_{\text{bulk}}$  record shows the same pattern for each of the three termination-interglacial  
180 transition: increases of 1 to 2‰ before the end of each termination (Fig 5), which translate to  
181 increases in nutrient utilization of 13-19% (TI to MIS 1), 20-26% (TII to MIS 5e) and 16-  
182 20% (TV to MIS 11). These estimates assume an classic isotope effect of 5 to 8 ‰ for nitrate  
183 assimilation (DiFiore et al., 2006). However, the shapes of the increases differ slightly in  
184 each period; the  $\delta^{15}N_{\text{bulk}}$  peak is already reached before the end of TI while it comes in the  
185 early or middle part of the interglacials during MIS 11 and 5e. While all interglacials are  
186 marked by the same pattern of enriched  $\delta^{15}N$  compared to their respective terminations, the  
187 average value is significantly different for each ( $2\sigma$ ,  $P < 0.0001$ , Kruskal-Wallis test  
188 performed with Prims6 software); the Holocene is the highest (~6.4 ‰,  $n = 23$ ) while the  
189 Eemian (~5.2 ‰  $n = 27$ ) and the Holsteinian (~4.8 ‰,  $n = 39$ ) are lower (Fig. 5). These  
190 translate to lower nitrate utilization rates of 13-19% (MIS 5e) and 17-25% (MIS 11)  
191 compared to the Holocene.

192

#### 193 *3.2. Potential alteration of $\delta^{15}N$*

194 Most of the  $\delta^{15}N_{\text{bulk}}$  values from the interglacial periods (Fig. 6) reflect the typical  
195 geochemical composition of marine algae (Meyers, 1997) , assuming a  $\delta^{15}N > 4.5\text{‰}$  for the  
196 regional oceanic nitrate pool (Sigman et al., 2009). That suggests a very low content of  
197 allochthonous (terrestrial) carbon-rich organic matter in the majority of the samples (Fig 6a),  
198 an observation consistent with C/N weight ratios that are  $<12$  (Fig. 6a). Moreover, the

199 relationship between the total organic carbon and total nitrogen contents (Fig 6b) yields a  
200 very small intercept (0.005), suggesting that the fraction of inorganic nitrogen in our  
201 samples— from for example, input of ammonium adsorbed into illite—is trivially small.  
202 Thus, while we can predict from (Fig 6a) that the terrestrial organic component is minimal for  
203 almost all samples, we also note that if diagenesis had significantly altered the nitrogen-  
204 bearing compounds in the deposits, there should be a relationship between the  $\delta^{15}\text{N}_{\text{bulk}}$  and  
205 the C/N ratio and total nitrogen. No such relationship is observed in the data (Fig 6a) or only  
206 weakly (6c). Futhermore, the C/N ratios of the three interglacial periods are very similar ( $P =$   
207 0.8189; Kruskal-Wallis test performed with Prims6 software), which argues against there  
208 being any major differences in either the source of nitrogen or alteration of nitrogen-bearing  
209 compounds between the interglacials. We therefore conclude that the  $\delta^{15}\text{N}_{\text{bulk}}$  values  
210 primarily reflect the  $\delta^{15}\text{N}$  of exported organic matter, assuming a constant diagenetic  
211 alteration through time (Robinson et al., 2012).

212

## 213 **4. Discussion**

### 214 *4.1. $\delta^{15}\text{N}_{\text{bulk}}$ variations from terminations to interglacial stages*

215 The  $\delta^{15}\text{N}$  of sinking organic matter is enriched during each interglacial relative to the  
216 preceding termination, being at least 1‰ higher during the Holocene compared to  
217 Termination 1, and ~2 ‰ higher between Termination II / MIS 5e and Termination V / MIS  
218 11 transitions. Similar enrichments in  $\delta^{15}\text{N}$  between the Last Glacial Maximum and the  
219 Holocene were previously observed in both the subpolar North Atlantic—using organic-  
220 bound  $\delta^{15}\text{N}$  of planktic foraminifera (Straub et al., 2013b)—and in the central Arctic using  
221  $\delta^{15}\text{N}_{\text{bulk}}$  (Schubert et al., 2001). In both regions, the increase in  $\delta^{15}\text{N}$  during the Holocene was  
222 attributed to more complete nitrate consumption due to a shallower summer mixed-layer, thus  
223 enhanced stratification.

224 While nitrate utilization is the most probable factor controlling  $\delta^{15}\text{N}$  in the polar  
225 region, another process could have induced changes: a varying rate of N fixation between  
226 glacial and interglacial times could have altered the nitrate  $\delta^{15}\text{N}$  of the surface nitrate pool.  
227 We can discount this potential influence as it has already been demonstrated that potential  
228 changes in N fixation are of the opposite sign required to explain observed variations in  $\delta^{15}\text{N}$   
229 during glacial-to-interglacial transitions (Ren et al., 2009; Straub et al., 2013a, 2013b).  
230 Moreover, we can also discount enhanced input of nitrate to surface waters during glacials as  
231 that would be associated with increased biogenic material fluxes during glacial episodes,  
232 which are not observed (Fig. 7), assuming that nitrate is the limiting during glacials as well.

233 Thus, we interpret the increase in  $\delta^{15}\text{N}_{\text{bulk}}$  during glacial-to-interglacial transitions as  
234 an indicator of a higher relative consumption of nitrate during the interglacial phase  
235 compared to the termination. This relationship holds for all three termination-to-interglacial  
236 intervals explored here (Fig. 7), and it highlights, for the first time, an apparent increase in  
237 nutrient utilization during each interglacial, most likely resulting from a thinner, well-  
238 illuminated summer mixed-layer. This is in accordance with results from the organic-bound  
239  $\delta^{15}\text{N}$  of planktic foraminifera and further illustrates that  $\delta^{15}\text{N}_{\text{bulk}}$  can record upper-ocean  
240 stratification under certain conditions.

241

#### 242 *4.2. Inter-interglacial $\delta^{15}\text{N}_{\text{bulk}}$ variations*

243 Within interglacials, we interpret differences in  $\delta^{15}\text{N}_{\text{bulk}}$  as reflecting changes in the  
244 relative nutrient utilization linked to different surface stratification conditions. Biogenic  
245 carbonate mass accumulation rates suggest that MIS 11 and MIS 5e were characterized by  
246 lower productivity; lower average  $\delta^{15}\text{N}_{\text{bulk}}$  assays during these times therefore do not reflect  
247 an enhanced supply of nitrate, which would have supported higher, not lower, productivity.  
248 The high mean  $\delta^{15}\text{N}_{\text{bulk}}$  value in the Holocene thus implies that during that epoch a more

249 stratified, more Atlantic-influenced oceanic structure with a very thin summer mixed-layer  
250 prevailed, conditions similar to those today (Fig 2). This hypothesis is supported by the  
251 decreasing interglacial dominance in our records of the polar foraminiferal species *NPs* (95 %  
252 average during MIS 11, 64 % during MIS 5e and only 44 % during the Holocene; Fig. 7). At  
253 face value the high percentages of *NPs* indicate that the water depth at which *NPs* usually  
254 resides was bathed in cold and relatively fresh polar water during the Holsteinian while  
255 higher proportions of warm, saltier Atlantic water were present at the same depth levels  
256 during the Eemian and, even more, during the Holocene.

257 Polar waters should be characterized by lighter oxygen isotope values but water  
258 temperature and ice-sheet volume also influence the *NPs* oxygen isotope signature and  
259 prevent a straightforward interpretation of the  $\delta^{18}\text{O}$  record. While our  $\delta^{18}\text{O}$  record is similar  
260 to the global  $\delta^{18}\text{O}$  stack and thus cannot be used to estimate with confidence the relative  
261 importance of freshwater release and temperature regionally (Fig 5), the shapes of the curves  
262 suggest a quite different timeline of events for each interglacial (Fig 8). For example, the  
263 inference that a deeper cold mixed-layer prevailed during MIS 11 and MIS 5e (Fig. 7) could  
264 be explained by a prolonged meltwater release from the surrounding ice-sheets that freshened  
265 the surface layer and forced the saltier Atlantic core to flow at a greater water depth (Bauch,  
266 2013; Van Nieuwenhove et al., 2011). This hypothesis is supported by the presence of IRD  
267 well into MIS 11 and, to a lesser extent, MIS 5e (Fig 7), and it is coherent with the  
268 hypothesized presence of an extremely large ice-sheet in MIS 12 (Rohling et al., 1998), that  
269 would have required a much longer time to completely melt. A change in the  $\delta^{15}\text{N}$  of the  
270 source nitrate could be proposed to justify the lower  $\delta^{15}\text{N}_{\text{bulk}}$  found for MIS 5e and MIS 11  
271 but this would not explain the higher abundance of *NPs* during those two intervals, both of  
272 which are typically reported as being warmer than the Holocene climate (Melles et al., 2012).  
273 The collective evidence therefore supports our hypothesis that the abundance of *NPs* does not

274 always relate directly to a more intense Atlantic Water inflow to the Nordic Seas but can be  
275 interpreted as reflecting the summer thickness of the cold mixed-layer and consequent  
276 changes in the depth of inflowing Atlantic Water. This hypothesis reconciles records  
277 suggesting a globally warmer-than-Holocene world with less ice over the high latitudes  
278 during MIS 5e and 11 (Bauch and Kandiano, 2007; de Vernal and Hillaire-Marcel, 2008;  
279 Melles et al., 2012; Otto-Bliesner et al., 2006; Vázquez Riveiros et al., 2013), with records  
280 indicating cooler SST in the Nordic seas and a low-saline halocline over the Vøring Plateau  
281 during the same intervals (Bauch et al., 2012; Kandiano et al., 2012; Van Nieuwenhove and  
282 Bauch, 2008) (Fig. 1). The deeper penetration depth of the Atlantic Water can also explain  
283 previously observed isotopically light benthic  $\delta^{18}\text{O}$  spikes or bottom water temperature  
284 variations during deglacial periods (Bauch et al., 2012, 2000; Rasmussen et al., 2003) as the  
285 Atlantic inflow might have been, at least partially, replaced by a very thick cold and fresh  
286 mixed layer, even at depth.

287

#### 288 *4.3. Intra-interglacial $\delta^{15}\text{N}_{\text{bulk}}$ variation*

289 In addition to differences in the average absolute value, each interglacial is unique in  
290 terms of  $\delta^{15}\text{N}_{\text{bulk}}$  variability. This implies short-lived episodes of relative nutrient utilization  
291 and water mass structure variability within the Nordic Seas during every warm interval.  
292 During Termination V and early MIS 11, high  $\delta^{15}\text{N}_{\text{bulk}}$  indicates that the upper layer of the  
293 Nordic Seas was dominated by a thick summer mixed-layer, which originated from the  
294 deglaciation following the extreme glacial conditions of MIS 12 (Rohling et al., 1998). The  
295 massively thick mixed-layer could have induced strong light limitation and low relative  
296 nutrient utilization initially, and later restrained advection of nutrients to the upper water,  
297 which contributed to the observed high  $\delta^{15}\text{N}_{\text{bulk}}$  toward the end of Termination V and its  
298 increase during the early phase of MIS 11 (Fig. 5). Coming off an intense glacial and a

299 Termination marked by an exceptionally long Heinrich-event-like stadial with a prolonged  
300 collapse of the AMOC (Vázquez Riveiros et al., 2013), the early  $\delta^{15}\text{N}_{\text{bulk}}$  peak and its  
301 subsequent high variability within the MIS 11 suggests a long period of surface water  
302 structure instability in the Nordic Seas during the entire interglacial (Fig. 7). Insolation  
303 changes were weak during the transition between MIS 12 and 11 and the observed variability  
304 in  $\delta^{15}\text{N}_{\text{bulk}}$  therefore highlights the sensitivity of upper ocean stratification in the Nordic Seas  
305 to other, non solar-related parameters such as input of meltwater and surface ocean current  
306 reorganization.

307 Termination II is also marked by low relative nitrate utilization due to the presence of  
308 the thick layer of meltwater caused by the deglaciation that could have induced light  
309 limitation during summer time. A subsequent and progressive increase in nitrate utilization  
310 abruptly stopped during the early Eemian as input of meltwater waned and the summer mixed  
311 layer shoaled. At this time, relative nitrate utilization suddenly decreased (Fig. 7). This  
312 minimum is synchronous with the minimum abundance of the subpolar planktic foraminifer  
313 *Globogerinita uvula* (Fig 7; Bauch et al., 2012) indicating the coldest conditions of the whole  
314 interglacial. The intense cooling can be linked to a southward shift of the polar front, which  
315 would have delivered fresh, cold water and created a thick, cold mixed-layer at the surface,  
316 thus limiting nitrate utilization. Finally, the increase in nitrate utilization seen in the early to  
317 Late Eemian data is interpreted to represent a transition from initially deeper stratification  
318 caused by meltwater originating from the early Eemian deglacial to a more Atlantic-  
319 influenced circulation mode (Fig. 7) in the Nordic seas (Bauch and Erlenkeuser, 2008; Van  
320 Nieuwenhove and Bauch, 2008). Toward the glacial inception in the later part of the Eemian,  
321 the decrease in  $\delta^{15}\text{N}_{\text{bulk}}$  to 5‰ reflects the progressive deepening of the summer mixed layer.

322 Like the previous terminations, a thick residual mixed-layer derived from the glacial  
323 period (Simstich et al., 2012) was present at the end of termination I. This quickly thinned



324 during the very early stage of the Holocene indicating a higher influence of Atlantic water at  
325 our site (Fig. 7). The plateau of high relative nitrate utilization persisted until the mid-  
326 Holocene where the sudden drop in  $\delta^{15}\text{N}_{\text{bulk}}$  is associated with a decrease in proportion of  
327 sub-polar foraminifera, indicating a thicker mixed-layer and a deeper Atlantic water inflow  
328 (Fig. 7). This sudden deepening of the mixed-layer might be linked to a sudden meltwater  
329 input or a southern shift of the East Greenland Current and it could be related to the so-called  
330 8.2 ka event (Alley et al., 1997). During the Holocene thermal optimum relative nitrate  
331 utilization is high and is accompanied by a strong presence of Atlantic-derived species (Fig.  
332 7), collectively indicating shoaling of the mixed-layer.

333

## 334 **5. Conclusions**

335 Our results support the hypothesis that nitrate utilization in the polar North Atlantic  
336 was lower during the last termination and subsequently increased at the beginning of the  
337 Holocene (Straub et al., 2013b). By extending the record to two older termination-interglacial  
338 periods within the Nordic Seas we have defined a similar pattern of steep increase in nitrate  
339 utilization. These results together imply a quick thinning of the summer mixed-layer at the  
340 beginning of interglacial periods, the likely cause being the accumulation of meltwater  
341 produced in the region during deglaciation. The potentially larger volume of meltwater  
342 discharged into the Nordic Seas well into MIS 11 explains why the summer mixed-layer  
343 thinning seems to have been relatively slowest during this period compared to the others.  
344 This is in agreement with our reconstructed summer mixed-layer depth during MIS 11, the  
345 thickest of the three interglacials studied here, which is consistent with the notion of the  
346 melting of an extremely large ice-sheet during Termination V (Rohling et al., 1998). The  
347 presence of a rather thick summer mixed-layer, and consequently a deeper Atlantic Water  
348 inflow, reconciles indications of a warmer general climate with the cooler SST in the Nordic

349 Seas during older interglacials (MIS 11 & 5e), compared to the Holocene (Fig 1). Moreover,  
350 it highlights that a thick summer mixed layer originating from the massive amount of  
351 freshwater water input that originated from the preceding glacial terminations did not inhibit  
352 the AMOC, since there is considerable evidence that AMOC was active throughout those  
353 interglacials (Bohm et al., 2015; Rodríguez-Tovar et al., 2015). Thus, the timing and location  
354 of important meltwater discharge events are probably the crucial factors in determining the  
355 effect of freshwater addition on the formation of deep-water. This new information needs to  
356 be considered when assessing the potential impact of the predicted demise of Greenland ice-  
357 sheet on regional oceanography.

358

### 359 **Acknowledgments:**

360 Data reported in the paper are available on Pangea  
361 (<https://doi.pangaea.de/10.1594/PANGAEA.805366>;[https://doi.pangaea.de/10.1594/PANGA](https://doi.pangaea.de/10.1594/PANGAEA.780099)  
362 [EA.780099](https://doi.pangaea.de/10.1594/PANGAEA.780099)). H.A.B., T.F.P. and B.T. developed the concept and designed the study. H.A.B.  
363 carried out samples preparation and contributed to the analysis. TFP thanks Kathy Gordon for  
364 conducting the nitrogen isotope measurements. B.T. interpreted the results and wrote the  
365 manuscript in collaboration with H.A.B. and T.F.P. Figure 1, 2 and 4 were created using  
366 Ocean Data View (Schlitzer, 2002). We are thankful to the editor H. Stoll and three  
367 anonymous reviewers for their comments and suggestions that improved the manuscript.

368

### 369 **References**

370

- 371 Alley, R.B., Mayewski, P.A., Sowers, T., Stuiver, M., Taylor, K.C., Clark, P.U., 1997.  
372 Holocene climatic instability: A prominent, widespread event 8200 yr ago. *Geology* 25,  
373 483.
- 374 Bauch, H.A., 2013. Interglacial climates and the Atlantic meridional overturning circulation:

- 375 is there an Arctic controversy? *Quat. Sci. Rev.* 63, 1–22.
- 376 Bauch, H.A., Erlenkeuser, H., 2008. A critical climatic evaluation of last interglacial (MIS  
377 5e) records from the Norwegian Sea. *Polar Res.* 27, 135–151.
- 378 Bauch, H.A., Erlenkeuser, H., Fahl, K., Spielhagen, R.F., Weinelt, M.S., Andruleit, H.,  
379 Henrich, R., 1999. Evidence for a steeper Eemian than Holocene sea surface  
380 temperature gradient between Arctic and sub-Arctic regions. *Palaeogeogr.*  
381 *Palaeoclimatol. Palaeoecol.* 145, 95–117.
- 382 Bauch, H.A., Erlenkeuser, H., Helmke, J.P., Struck, U., 2000. A paleoclimatic evaluation of  
383 marine oxygen isotope stage 11 in the high-northern Atlantic (Nordic seas). *Glob.*  
384 *Planet. Change* 24, 27–39.
- 385 Bauch, H.A., Erlenkeuser, H., Spielhagen, R.F., Struck, U., Matthiessen, J., Thiede, J.,  
386 Heinemeier, J., 2001. A multiproxy reconstruction of the evolution of deep and surface  
387 waters in the subarctic Nordic seas over the last 30,000 yr. *Quat. Sci. Rev.* 20, 659–678.
- 388 Bauch, H.A., Kandiano, E.S., 2007. Evidence for early warming and cooling in North  
389 Atlantic surface waters during the last interglacial. *Paleoceanography* 22, PA1201.
- 390 Bauch, H.A., Kandiano, E.S., Helmke, J.P., 2012. Contrasting ocean changes between the  
391 subpolar and polar North Atlantic during the past 135 ka. *Geophys. Res. Lett.* 39.
- 392 Bauch, H.A., Struck, U., Thiede, J., 2001. Planktic and benthic foraminifera as indicators for  
393 past ocean changes in surface and deep waters of the Nordic seas. *North. North Atl. a*  
394 *Chang. Environ.*
- 395 Berger, A., Loutre, M.F., 1991. Insolation values for the climate of the last 10 million years.  
396 *Quat. Sci. Rev.* 10, 297–317.
- 397 Bohm, E., Lippold, J., Gutjahr, M., Frank, M., Blaser, P., Antz, B., Fohlmeister, J., Frank, N.,  
398 Andersen, M.B., Deininger, M., 2015. Strong and deep Atlantic meridional overturning  
399 circulation during the last glacial cycle. *Nature* 517, 73–76.
- 400 CAPE Last Interglacial Project Members, 2006. Last Interglacial Arctic warmth confirms  
401 polar amplification of climate change. *Quat. Sci. Rev.* 25, 1383–1400.
- 402 Clark, P.U., Pisias, N.G., Stocker, T.F., Weaver, A.J., 2002. The role of the thermohaline  
403 circulation in abrupt climate change. *Nature* 415, 863–9.
- 404 de Vernal, A., Hillaire-Marcel, C., 2008. Natural variability of Greenland climate, vegetation,  
405 and ice volume during the past million years. *Science* 320, 1622–5.
- 406 Dickson, R., Rudels, B., Dye, S., Karcher, M., Meincke, J., Yashayaev, I., 2007. Current  
407 estimates of freshwater flux through Arctic and subarctic seas. *Prog. Oceanogr.* 73, 210–  
408 230.
- 409 DiFiore, P.J., Sigman, D.M., Trull, T.W., Lourey, M.J., Karsh, K., Cane, G., Ho, R., 2006.  
410 Nitrogen isotope constraints on subantarctic biogeochemistry. *J. Geophys. Res.* 111,  
411 C08016.
- 412 EPICA community members, 2004. Eight glacial cycles from an Antarctic ice core. *Nature*  
413 429, 623–8.
- 414 Fronval, T., Jansen, E., 1996. Rapid changes in ocean circulation and heat flux in the Nordic  
415 seas during the last interglacial period. *Nature* 383, 806–810.

- 416 Galaasen, E.V., Ninnemann, U.S., Irvalı, N., Kleiven, H.K.F., Rosenthal, Y., Kissel, C.,  
417 Hodell, D.A., 2014. Rapid reductions in North Atlantic Deep Water during the peak of  
418 the last interglacial period. *Science* 343, 1129–32.
- 419 Galbraith, E.D., Sigman, D.M., Robinson, R.S., Pedersen, T.F., 2008. Nitrogen in Past  
420 Marine Environments.
- 421 Glessmer, M.S., Eldevik, T., Våge, K., Øie Nilsen, J.E., Behrens, E., 2014. Atlantic origin of  
422 observed and modelled freshwater anomalies in the Nordic Seas. *Nat. Geosci.* 7, 801–  
423 805.
- 424 Hansen, B., Østerhus, S., 2000. North Atlantic-Nordic Seas exchanges. *Prog. Oceanogr.*
- 425 Isachsen, P.E., Mauritzen, C., Svendsen, H., 2007. Dense water formation in the Nordic Seas  
426 diagnosed from sea surface buoyancy fluxes. *Deep Sea Res. Part I Oceanogr. Res. Pap.*  
427 54, 22–41.
- 428 Jeansson, E., Bellerby, R.G.J., Skjelvan, I., Frigstad, H., Ólafsdóttir, S.R., Olafsson, J., 2015.  
429 Fluxes of carbon and nutrients to the Iceland Sea surface layer and inferred primary  
430 productivity and stoichiometry. *Biogeosciences* 12, 875–885.
- 431 Kandiano, E.S., Bauch, H.A., Fahl, K., Helmke, J.P., Röhl, U., Pérez-Folgado, M., Cacho, I.,  
432 2012. The meridional temperature gradient in the eastern North Atlantic during MIS 11  
433 and its link to the ocean–atmosphere system. *Palaeogeogr. Palaeoclimatol. Palaeoecol.*  
434 333–334, 24–39.
- 435 Kaspar, F., 2005. A model-data comparison of European temperatures in the Eemian  
436 interglacial. *Geophys. Res. Lett.* 32, L11703.
- 437 Kirtman, B., Power, S.B., Adedoyin, J.A., Boer, G.J., Bojariu, R., Camilloni, I., Doblas-  
438 Reyes, F.J., Fiore, A.M., Kimoto, M., Meehl, G.A., Prather, M., Sarr, A., Schär, C.,  
439 Sutton, R., Van Oldenborgh, G.J., Vecchi, G., Wang, H.J., 2013. Near-term Climate  
440 Change: Projections and Predictability. In: Stocker, T.F., Qin, D., Plattner, G.-K.,  
441 Tignor, M., Allen, S.K., Boschung, J., Nauels, A., Xia, Y., Bex, V., Midgley, P.M.  
442 (Eds.), *Climate Change 2013: The Physical Science Basis. Contribution of Working*  
443 *Group I to the Fifth Assessment Report of the Intergovernmental Panel on Climate*  
444 *Change.* Cambridge University Press, Cambridge, United Kingdom and New York, NY,  
445 USA, pp. 953–1028.
- 446 Lisiecki, L.E., Raymo, M.E., 2005. A Pliocene-Pleistocene stack of 57 globally distributed  
447 benthic  $\delta^{18}\text{O}$  records. *Paleoceanography* 20, 1–17.
- 448 Lohmann, K., JungCLAUS, J.H., Matei, D., Mignot, J., Menary, M., Langehaug, H.R., Ba, J.,  
449 Gao, Y., Otterå, O.H., Park, W., Lorenz, S., 2014. The role of subpolar deep water  
450 formation and Nordic Seas overflows in simulated multidecadal variability of the  
451 Atlantic meridional overturning circulation. *Ocean Sci.* 10, 227–241.
- 452 Lynch-Stieglitz, J., Adkins, J.F., Curry, W.B., Dokken, T., Hall, I.R., Herguera, J.C., Hirschi,  
453 J.J.-M., Ivanova, E. V., Kissel, C., Marchal, O., Marchitto, T.M., McCave, I.N.,  
454 McManus, J.F., Mulitza, S., Ninnemann, U., Peeters, F., Yu, E.-F., Zahn, R., 2007.  
455 Atlantic meridional overturning circulation during the Last Glacial Maximum. *Science*  
456 316, 66–9.
- 457 Mauritzen, C., 1996. Production of dense overflow waters feeding the North Atlantic across  
458 the Greenland-Scotland Ridge. Part 1: Evidence for a revised circulation scheme. *Deep*  
459 *Sea Res. Part I Oceanogr. Res. Pap.* 43, 769–806.

- 460 Melles, M., Brigham-Grette, J., Minyuk, P.S., Nowaczyk, N.R., Wennrich, V., DeConto,  
461 R.M., Anderson, P.M., Andreev, A.A., Coletti, A., Cook, T.L., Haltia-Hovi, E.,  
462 Kukkonen, M., Lozhkin, A. V, Rosén, P., Tarasov, P., Vogel, H., Wagner, B., 2012. 2.8  
463 million years of Arctic climate change from Lake El'gygytgyn, NE Russia. *Science* 337,  
464 315–20.
- 465 Meyers, P.A., 1997. Organic geochemical proxies of paleoceanographic, paleolimnologic,  
466 and paleoclimatic processes. *Org. Geochem.* 27, 213–250.
- 467 Otto-Bliesner, B.L., Marshall, S.J., Overpeck, J.T., Miller, G.H., Hu, A., 2006. Simulating  
468 Arctic climate warmth and icefield retreat in the last interglaciation. *Science* 311, 1751–  
469 3.
- 470 Pados, T., Spielhagen, R.F., 2014. Species distribution and depth habitat of recent planktic  
471 foraminifera in Fram Strait, Arctic Ocean. *Polar Res.* 33.
- 472 Peterson, B.J., McClelland, J., Curry, R., Holmes, R.M., Walsh, J.E., Aagaard, K., 2006.  
473 Trajectory Shifts in the Arctic and Subarctic Freshwater Cycle. *Sci.* 313, 1061–1066.
- 474 Rahmstorf, S., 2002. Ocean circulation and climate during the past 120,000 years. *Nature*  
475 419, 207–14.
- 476 Rahmstorf, S., Box, J.E., Feulner, G., Mann, M.E., Robinson, A., Rutherford, S.,  
477 Schaffernicht, E.J., 2015. Exceptional twentieth-century slowdown in Atlantic Ocean  
478 overturning circulation. *Nat. Clim. Chang.* 5, 475–480.
- 479 Rasmussen, T.L., Thomsen, E., Kuijpers, A., Wastegård, S., 2003. Late warming and early  
480 cooling of the sea surface in the Nordic seas during MIS 5e (Eemian Interglacial). *Quat.*  
481 *Sci. Rev.* 22, 809–821.
- 482 Ren, H., Sigman, D.M., Meckler, A.N., Plessen, B., Robinson, R.S., Rosenthal, Y., Haug,  
483 G.H., 2009. Foraminiferal isotope evidence of reduced nitrogen fixation in the ice age  
484 Atlantic Ocean. *Science* 323, 244–8.
- 485 Robinson, R.S., Kienast, M., Luiza Albuquerque, A., Altabet, M., Contreras, S., De Pol Holz,  
486 R., Dubois, N., Francois, R., Galbraith, E., Hsu, T.C., Ivanochko, T., Jaccard, S., Kao,  
487 S.J., Kiefer, T., Kienast, S., Lehmann, M., Martinez, P., McCarthy, M., M??bius, J.,  
488 Pedersen, T., Quan, T.M., Ryabenko, E., Schmittner, A., Schneider, R., Schneider-Mor,  
489 A., Shigemitsu, M., Sinclair, D., Somes, C., Studer, A., Thunell, R., Yang, J.Y., 2012. A  
490 review of nitrogen isotopic alteration in marine sediments. *Paleoceanography*.
- 491 Rodríguez-Tovar, F.J., Dorador, J., Martin-Garcia, G.M., Sierro, F.J., Flores, J.A., Hodell,  
492 D.A., 2015. Response of macrobenthic and foraminifer communities to changes in deep-  
493 sea environmental conditions from Marine Isotope Stage (MIS) 12 to 11 at the  
494 “Shackleton Site.” *Glob. Planet. Change* 133, 176–187.
- 495 Rohling, E.J., Fenton, M., Jorissen, F.J., Bertrand, P., Ganssen, G., Caulet, J.P., 1998.  
496 Magnitudes of sea-level lowstands of the past 500,000 years. *Nature* 394, 162–165.
- 497 Schlitzer, R., 2002. Interactive analysis and visualization of geoscience data with Ocean Data  
498 View. *Comput. Geosci.* 28, 1211–1218.
- 499 Schubert, C.J., Stein, R., Calvert, S.E., 2001. Tracking nutrient and productivity variations  
500 over the Last Deglaciation in the Arctic Ocean. *Paleoceanography* 16, 199–211.
- 501 Seidenkrantz, M.S., Kristensen, P., Knudsen, K.L., 1995. Marine evidence for climatic  
502 instability during the last interglacial in shelf records from northwest Europe. *J. Quat.*

- 503           Sci.
- 504   Sigman, D.M., Difiore, P.J., Hain, M.P., Deutsch, C., Wang, Y., Karl, D.M., Knapp, A.N.,  
505       Lehmann, M.F., Pantoja, S., 2009. Deep-Sea Research I The dual isotopes of deep  
506       nitrate as a constraint on the cycle and budget of oceanic fixed nitrogen. *Deep. Res. Part*  
507       I 56, 1419–1439.
- 508   Simstich, J., Lorenz, S.J., Bauch, H.A., 2012. Evaluation of past stratification changes in the  
509       Nordic Seas by comparing planktonic foraminiferal  $\delta^{18}\text{O}$  with a solar-forced model.  
510       *Mar. Micropaleontol.* 94–95, 91–96.
- 511   Straub, M., Sigman, D.M., Ren, H., Martinez-Garcia, A., Meckler, A.N., Hain, M.P., Haug,  
512       G.H., 2013a. Changes in North Atlantic nitrogen fixation controlled by ocean  
513       circulation. *Nature* 501, 200–+.
- 514   Straub, M., Tremblay, M.M., Sigman, D.M., Studer, A.S., Ren, H., Toggweiler, J.R., Haug,  
515       G.H., 2013b. Nutrient conditions in the subpolar North Atlantic during the last glacial  
516       period reconstructed from foraminifera-bound nitrogen isotopes. *Paleoceanography* 28,  
517       79–90.
- 518   Swift, J.H., Aagaard, K., 1981. Seasonal transitions and water mass formation in the Iceland  
519       and Greenland seas. *Deep Sea Res. Part A. Oceanogr. Res. Pap.* 28, 1107–1129.
- 520   Van Nieuwenhove, N., Bauch, H.A., 2008. Last interglacial (MIS 5e) surface water  
521       conditions at the Vring Plateau (Norwegian Sea), based on dinoflagellate cysts. *Polar*  
522       *Res.* 27, 175–186.
- 523   Van Nieuwenhove, N., Bauch, H.A., Eynaud, F., Kandiano, E., Cortijo, E., Turon, J.-L.,  
524       2011. Evidence for delayed poleward expansion of North Atlantic surface waters during  
525       the last interglacial (MIS 5e). *Quat. Sci. Rev.* 30, 934–946.
- 526   Vázquez Riveiros, N., Waelbroeck, C., Skinner, L., Duplessy, J.-C., McManus, J.F.,  
527       Kandiano, E.S., Bauch, H.A., 2013. The “MIS 11 paradox” and ocean circulation: Role  
528       of millennial scale events. *Earth Planet. Sci. Lett.* 371–372, 258–268.
- 529   Vellinga, M., Wood, R.A., 2002. Global climatic impacts of a collapse of the atlantic  
530       thermohaline circulation. *Clim. Change* 54, 251–267.
- 531
- 532

533

534 **Fig. 1.** Heat distribution within the Nordic Seas during interglacials. Comparison of averaged  
535 alkenone-derived sea surface temperature reconstruction (Kandiano et al., 2012; Van  
536 Nieuwenhove et al., 2011) during MIS 1 and MIS 11 (note that core PS1243 [this study] and  
537 MD99-2277 were retrieve from approximately the same site). Color of the dots represent  
538 alkenone-derived sea surface temperature. Gray scale represent bathymetry.

539

540 **Fig 2.** Modern seasonal upper-ocean temperature structure and dissolved nitrate content of  
541 surface waters and the upper-water column the Nordic Seas with the location of the mixed-  
542 layer. The star represents our coring site.

543

544 **Fig 3.** Conceptual relationships among nitrate utilization,  $\delta^{15}\text{N}$  of exported organic matter  
545 and abundance of *Neogloboquadrina pachyderma* sinistral (*NPs*), with respect to the  
546 thickness of the summer mixed-layer (light blue).

547

548 **Fig. 4.** Water-mass and temperature distributions as a function of depth in the Nordic Sea  
549 region. The core location north of Iceland is shown by the black star.

550

551 **Fig 5.** Data from core PS1243 plotted against age and compared to global  $\delta^{18}\text{O}$  stack in black  
552 (Lisiecki and Raymo, 2005). Complete  $\delta^{18}\text{O}$  *NPs*,  $\delta^{15}\text{N}_{\text{bulk}}$ , *NPs*, IRD record and carbonate  
553 content and accumulation rate are plotted in function of age (ky) for core PS1243 (top). The  
554 pale blue bars represent terminations, while the vertical yellow bars represent interglacial  
555 intervals. The bottom panel is a close-up of the radiocarbon dated part of the core.

556

557 **Fig. 6.** Relationships among  $\delta^{15}\text{N}_{\text{bulk}}$ , total N and C contents and the C/N weight ratio in the  
558 deposits. The colors define specific interglacial stages.

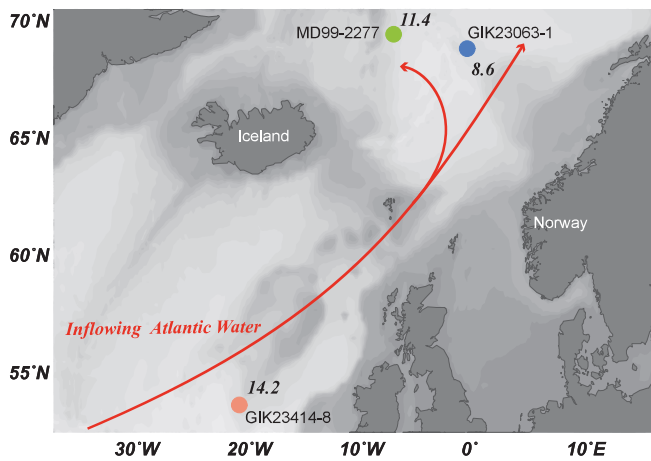
559

560 **Fig. 7.** Stratification during interglacial and termination. Interglacial and termination  $\delta^{18}\text{O}$   
561  $\text{NPs}$ ,  $\delta^{15}\text{N}_{\text{bulk}}$ ,  $\text{NPs}$ , *G. uvula* and *T. quiqueloba* abundance, carbonate content and  
562 accumulation rate and IRD record are plotted in function of age (ky) for core PS1243 (top)  
563 along our  $\delta^{15}\text{N}_{\text{bulk}}$  and  $\text{NPs}$ -based qualitative estimate of mixed-layer depth (bottom). Our  
564 mixed-layer depth estimate represents only the general trend for each interglacial without the  
565 inclusion of short-lived episodes and aims at visualizing the differences in the mixed-layer  
566 thickness variability and its impact on our proxies in each period.

567



### MIS 1



### MIS 11

